Science of the Total Environment 691 (2019) 516–527

Contents lists available at ScienceDirect

Science of the Total Environment

journal homepage: www.elsevier.com/locate/scitotenv

Toward stomatal–flux based forest protection against ozone: The MOTTLES approach

E. Paoletti [a], A. Alivernini [b], A. Anav [a,e], O. Badea [c], E. Carrari [a,*], S. Chivulescu [c], A. Conte [b], M.L. Ciriani [d], L. Dalstein-Richier [d], A. De Marco [e], S. Fares [b], G. Fasano [a], A. Giovannelli [a], M. Lazzara [a], S. Leca [c], A. Materassi [a], V. Moretti [b], D. Pitar [c], I. Popa [c], F. Sabatini [a], L. Salvati [b], P. Sicard [f], T. Sorgi [b], Y. Hoshika [a]

[a] CNR, Via Madonna del Piano 10, 50019 Sesto Fiorentino, Italy
[b] CREA – Research Centre for Forestry and Wood, Viale S. Margherita 80, 52100 Arezzo, Italy
[c] INCDS, 128 Eroilor Bvd., 077030 Voluntari, Romania
[d] GIEFS, 69 avenue des Hespérides, 06300 Nice, France
[e] ENEA, SSPT–PVS, Via Anguillarese 301, 00123 Santa Maria di Galeria (Rome), Italy
[f] ARGANS, 260 route du Pin Montard, 06410 Biot, France

HIGHLIGHTS

- The MOTTLES network for active O_3 monitoring in forests is described.
- In 2017, AOT40 exceeded twice the limit of the European Directive for forests.
- O_3 metrics from European protocols were representative of actual exposure/fluxes.
- AOT40 and PODy were inversely correlated.
- Visible foliar injury was the best forest–health indicator for O_3.

ARTICLE INFO

Article history:
Received 21 February 2019
Received in revised form 27 June 2019
Accepted 30 June 2019
Available online 2 July 2019

Editor: Dr. Jay Gan

Keywords:
Ground–level ozone
Forest monitoring
O_3 injury
O_3 metrics
Forest health indicators

ABSTRACT

European standards for the protection of forests from ozone (O_3) are based on atmospheric exposure (AOT40) that is not always representative of O_3 effects since it is not a proxy of gas uptake through stomata (stomatal flux). MOTTLES "*MOnitoring ozone injury for seTTing new critical LEvelS*" is a LIFE project aimed at establishing a permanent network of forest sites based on active O_3 monitoring at remote areas at high and medium risk of O_3 injury, in order to define new standards based on stomatal flux, i.e. POD_Y (Phytotoxic Ozone Dose above a threshold Y of uptake). Based on the first year of data collected at MOTTLES sites, we describe the MOTTLES monitoring station, together with protocols and metric calculation methods. AOT40 and POD_Y, computed with different methods, are then compared and correlated with forest–health indicators (radial growth, crown defoliation, visible foliar O_3 injury). For the year 2017, the average AOT40 calculated according to the European Directive was even 5 times (on average 1.7 times) the European legislative standard for the protection of forests. When the metrics were calculated according to the European protocols (EU Directive 2008/50/EC or Modelling and Mapping Manual LTRAP Convention), the values were well correlated to those obtained on the basis of the real duration of the growing season (i.e. MOTTLES method) and were thus representative of the actual exposure/flux. AOT40 showed opposite direction relative to PODY. Visible foliar O_3 injury appeared as the best forest–health indicator for O_3 under field conditions and was more frequently detected at forest edge than inside the forest. The present work may help the set–up of further long–term forest monitoring sites dedicated to O_3 assessment in forests, especially because flux-based assessments are recommended as part of monitoring air pollution impacts on ecosystems in the revised EU National Emissions Ceilings Directive.

1. Introduction

Tropospheric ozone (O_3) is a secondary photochemical air pollutant and a major air quality issue over large regions of the globe (Lefohn

* Corresponding author.
E-mail address: elisa.carrari@ipsp.cnr.it (E. Carrari).

https://doi.org/10.1016/j.scitotenv.2019.06.525
0048-9697/

et al., 2010; Mills et al., 2011; Langner et al., 2012; Cooper et al., 2014; Sicard et al., 2016a,b; Mills et al., 2018). Current surface O_3 levels are considered high enough to damage plants and thus reduce growth and productivity (Proietti et al., 2016; Li et al., 2018; Mills et al., 2018). To assess the potential O_3 risk to vegetation, several metrics have been developed (Paoletti and Manning, 2007; Lefohn et al., 2018). The European Community (EC) legislative standard is AOT40, i.e. the accumulation of O_3 concentrations exceeding 40 ppb over daylight hours (8 AM–8 PM) from April to September (EU Directive 2008/50/EC). AOT40 assumes that the damage to vegetation depends only on the atmospheric O_3 concentrations, while O_3 can damage the plants when absorbed through the stomata (Paoletti and Manning, 2007). This is why a new metric has been proposed, i.e. the phytotoxic ozone dose (POD_Y), defined as the accumulated O_3 flux entering into the leaves via the stomata, over a detoxification threshold Y (Emberson et al., 2000; Mills et al., 2011). The exceedances of POD_Y critical levels (CLs), together with visible foliar O_3 injury, are now recommended as indicators in the revised National Emission Ceilings (NEC) Directive (2016/2284 on the reduction of national emissions of certain atmospheric pollutants). EU Member States shall monitor the impacts of air pollution (including O_3) on ecosystems, based on a network of monitoring sites representative of their habitats. Site–specific POD_Y values can be calculated on the basis of measured O_3 concentrations, meteorology (temperature, relative humidity, light intensity, soil moisture, wind speed, atmospheric pressure) and soil type at or near the site, according to the DO_3SE model (CLRTAP, 2017). Following the revision of the NEC Directive, the interest in calculating POD_Y based on site-specific monitoring might increase in Europe (De Marco et al., 2019).

Epidemiological observation of O_3–induced injury and environmental variables, including O_3, can be used to derive CLs for forest protection under natural field conditions (Sicard et al., 2016a). Epidemiology is defined as the study of the factors affecting the frequency and distribution of diseases, injury, and other health–related events in a specified population for the purpose of establishing prevention and control programs (Braun et al., 2017). Many plant species respond to ambient O_3 pollution with O_3–specific visible foliar injury that can be diagnosed in the field (Paoletti et al., 2009; Sicard et al., 2016a; Li et al., 2018). The visible foliar O_3 injury on needles and leaves is the only evidence that can be visually detected in the field by experts without the support of instruments, and is included in the European monitoring programs for forest protection against O_3 pollution (Schaub et al., 2016). Another plant–response indicator for forest health is crown defoliation (Badea et al., 2004). Recent studies provided statistical evidence that O_3 has a negative impact on crown defoliation, both in Southern Europe (Díaz-de-Quijano et al., 2009; Sicard and Dalstein–Richier, 2015) and in countries where the AOT40 values for forests are usually lower than in European southern countries, e.g. Lithuania (Augustaitis and Bytnerowicz, 2008; Girgždienė et al., 2009; Augustaitis et al., 2010; Araminiene et al., 2019) or Romania (De Marco et al., 2017). Ozone can also affect forest growth (McLaughlin et al., 2007; Matyssek et al., 2010; Braun et al., 2017). We know that interactions between ambient O_3 and climate are expected to be important modifiers of future forest growth (McLaughlin and Downing, 1996). However, the separation of the impact of O_3 on tree growth in mature forests from other disturbances is challenging and requires long-term monitoring which has been missing so far.

The MOTTLES project, started in July 2016, implemented a permanent new–generation monitoring system with 17 forest sites at high and medium risk of O_3 injury in France, Italy and Romania. Each site is equipped with an active O_3 monitor and a meteorological station (including soil water content), that record variables at the 1-h temporal resolution needed to compute stomatal O_3 flux (POD_Y). In parallel, MOTTLES assesses forest–health indicators, i.e. visible foliar O_3 injury (once a year), crown defoliation (once a year) and radial growth (continuously, averaged at 1-h intervals), in order to estimate new POD_Y–based CLs.

Based on the first-year MOTTLES measurements, this paper aims to: 1. propose the set–up of the MOTTLES network as an example for an epidemiological assessment of POD_Y–based CLs in forests, and 2. clarify which O_3 metric and forest–health indicator are better suited for monitoring O_3 injury in real–world forests. We hypothesized that AOT40 and POD1 are uncoupled, and that the best forest–health indicator for O_3 damage under field conditions is visible foliar O_3 injury.

2. Methods

2.1. Setting–up the monitoring network

Seventeen forest sites were selected in France, Italy and Romania, from main European networks involved in air–quality monitoring (MERA in France and ICP Forests in Italy and Romania). Visits to the selected plots were carried out in summer 2016 in order to check ecological characteristics and status of the meteorological stations. Selection was based on type of vegetation (representative of main biogeographical regions) and exposure to a range of O_3 pollution, and resulted in 9 sites in Italy, 4 in France and 4 in Romania (Fig. 1, Table 1). The network covers large soil and climatic gradients, four biogeographical areas (Atlantic, Alpine, Continental and Mediterranean) and major forest types of Europe, extending from the schlerophyll forests of the Mediterranean area at Castelporziano (Italy) to the mountainous beech forests of the Alpine region of Romania. The mean annual temperatures range from ca. 2 °C in Fundata (Romania) to ca. 17 °C in Castelporziano (Italy) (Table 2). The network hosts 11 target species (7 broadleaved and 4 coniferous).

Following recommendations of the ICP Forests monitoring (Ferretti et al., 2017), meteorological and O_3 values are recorded in open areas (*open field*–OFD), while soil moisture and forest–health indicators are recorded into the forest (*in the plot*–ITP) (Fig. 2). Therefore, all sites are equipped with one OFD station and a nearby ITP station. The average distance between OFD and ITP is 600 m. Each OFD station is equipped with sensors for rainfall, air temperature, relative humidity, air pressure, solar radiation, wind speed and direction (DeltaOHM, Italy), while surface O_3 is measured by an active monitor (Model 106–L, 2B Technologies, Inc., Boulder, Colorado, USA). All sensors are installed at 2 m above ground level (Fig. 2). Each ITP station is equipped with soil moisture and soil temperature sensors (Campbell Scientific; USA/UK) placed at 10 cm depth, randomly located by avoiding areas around tree stems (1 m) or other disturbances, and a minimum of 4 point dendrometers installed on dominant or co–dominant trees chosen among individuals of the target tree species, in order to measure the same trees also evaluated for crown defoliation (see Section 2.3.2).. The target species are the most abundant tree species at each site. Data acquisition interval varies from 10 s to 15 min depending on the sensor, and the average is stored every hour as required for POD_Y calculation. Data acquisition is based on data loggers (Campbell Scientific; USA/UK) equipped with a custom–made program. Power supply is assured by solar panels or mains, when present, and backup batteries. Where GPRS connection is available, data are transmitted to an FTP server. In case of transmission failure, the data–logger memory ensures the integrity of acquired data so that the acquisition continues without interruption. Where GPRS is not available (e.g. the four French sites), a manual downloading by local site managers is conducted weekly and all data are sent by email to the data manager. A first data validation is made by the data acquisition systems on instantaneous values before averaging; a further validation is done on the rough data at the FTP server of each country before transferring from the national dataset to the MOTTLES FTP.

Data recording started between March and September 2017 (Table 1). Results are presented here for sites with at least 75% availability of hourly O_3 data in 2017 (calculated on the basis of the accumulation period).

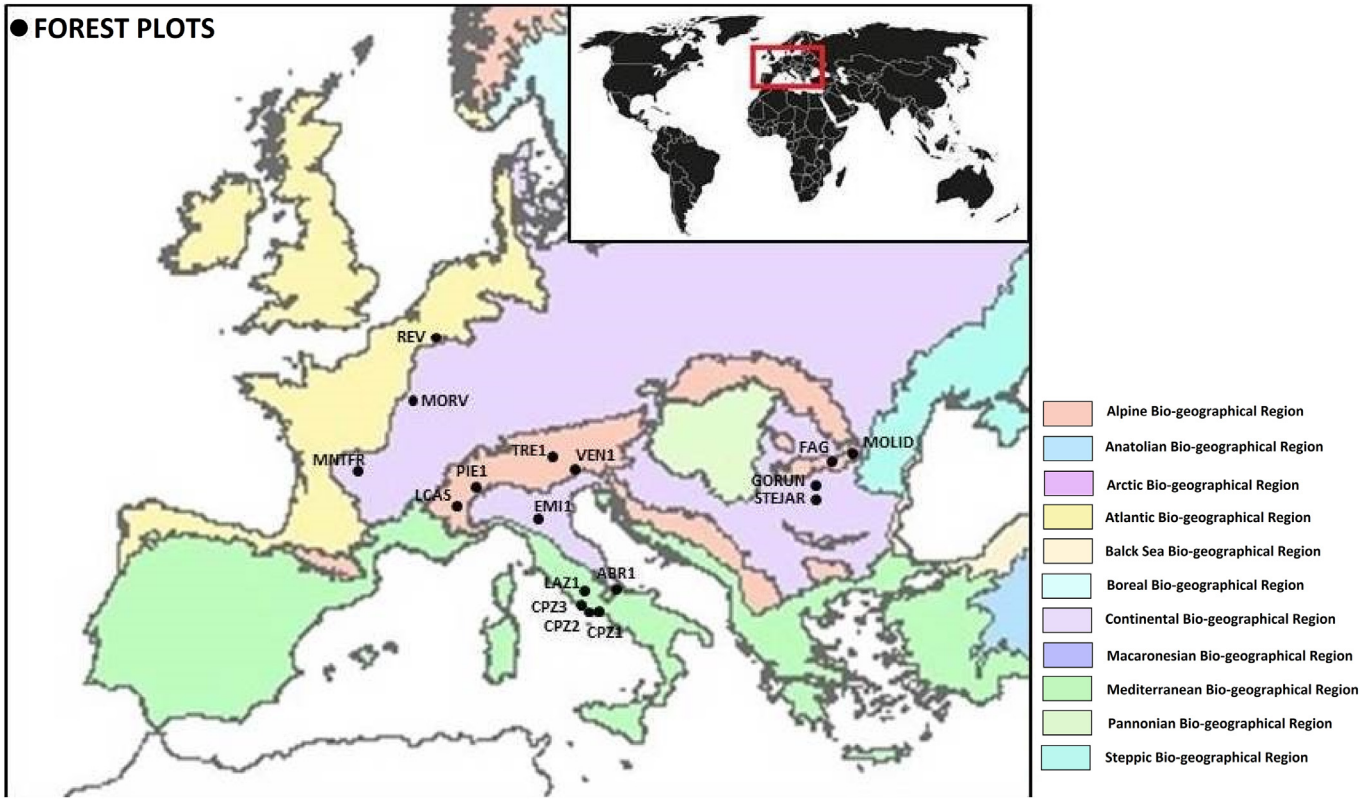

Fig. 1. Map of the MOTTLES forest site network across three countries (France, Italy, Romania) and four biogeographical regions (Atlantic, continental, Mediterranean, alpine).

2.2. Ozone metrics

2.2.1. Calculation of AOT40

AOT40 (in ppb h) was calculated as the sum of the hourly exceedances above 40 ppb, for daylight hours (for simplicity 8–20 Central European Time, CET) during the time window recommended by the EC Directive 2008/50/EC for forests i.e. April 1st to September 30th. It is worth noting that this accumulation time window for forests is mentioned in the footnote of the criteria in Section A.2 of Annex VII of the Directive, while a time window from May 1st to July 31st is mentioned in the main text.

$$AOT40_{Directive} = \int_{t=01April}^{30September} \max([O_3]-40, 0) \cdot dt \quad (1)$$

where $[O_3]$ is the measured hourly O_3 concentration (ppb) and dt is time step (1-h).

AOT40 was also calculated over the growing seasons recommended by ICP Vegetation for deciduous forest broadleaf and Alpine/Continental conifer trees, i.e. April 1st to September 30th, or for Mediterranean evergreen trees, i.e. year–long, during the daylight hours when global radiation is higher than 50 W m^{-2} (CLRTAP, 2017)

$$AOT40_{ICP} = \int_{t=SGS}^{EGS} \max([O_3]-40, 0) \cdot dt \quad (2)$$

where SGS is the start day of the year (DOY) of the growing season (January 1st or April 1st) and EGS is the end DOY of the growing season (December 31st or September 30th) depending whether the dominant tree species at each site is a Mediterranean conifer or not, respectively.

Based on the phenological assessments carried out by MOTTLES surveyors, SGS and EGS were also assessed (see Section 2.2.2.2); thus, AOT40 was also cumulated along the actual growing season of the dominant tree species at each site:

$$AOT40_{MOTTLES} = \int_{t=aSGS}^{aEGS} \max([O_3]-40, 0) \cdot dt \quad (3)$$

where aSGS and aEGS are the actual start and end of the growing season. However, the visible injury survey was not carried out at the very end of the growing season, when visible foliar O_3 injury may be masked by leaf senescence (Tagliaferro et al., 2005; Schaub et al., 2010). Therefore, we considered also an accumulation period starting from aSGS until the day when the survey of forest-health responses was carried out at a site, i.e.:

$$AOT40_{Survey} = \int_{t=aSGS}^{Survey\ date} \max([O_3]-40, 0) \cdot dt \quad (4)$$

The Directive 2008/50/EC requires >90% of validated 1-h O_3 concentration values over the defined time–window for calculating AOT40. For the first year of MOTTLES, we decided to use no gap filling procedure, while we used a less restrictive threshold of 75% of validated 1-h O_3 concentration values.

2.2.2. Estimation of POD_Y

POD_Y was estimated by extrapolating the values measured at 2 m a.g.l. up to the actual crown height, as recommended by the Manual on Methodologies and Criteria for Modelling and Mapping Critical Loads and Levels and Air Pollution Effects, Risks and Trends (CLRTAP, 2017). Within MOTTLES, we are able to evaluate any possible Y threshold for effects on forest–health indicators. Here, however, we present only the results of Y = 1, as recommended by CLRTAP (2017).

Similarly to what was done for AOT40, POD1 was accumulated over the period recommended by the European Directive 2008/50/EC

Table 1
Main characteristics of the forest sites included in the MOTTLES network.

Site	Code	Country	Latitude, N[a]	Longitude, E[a]	Altitude m a.s.l.	Dominant species	Slope and aspect	Parent rock	Soil type[b]	Biogeographical area[c]	Start of O_3 recording
Le Casset	LCAS	France	44.99703	6.48802	1755	*Larix decidua*	30° E	Glacial moraine, limestone	*Orthic Luvisols*	Alpine	01/04/2017
Montfranc	MNTFR	France	45.80500	2.06200	810	*Pinus sylvestris*	Plain	Brunisol – silt loam	*Dystric Cambisols*	Continental	01/04/2017
Morvan	MORV	France	47.27491	4.09921	620	*Alnus glutinosa*	6.5° SE	Brunisol – loam, overlying a granitic saprolite	*Chromic Cambisols*	Continental	01/04/2017
Revin	REV	France	49.90778	4.62972	390	*Picea abies*	2°	Silt loam	*Calcaric Leptosol*	Atlantic–Continental	21/03/2017
Selva Piana	ABR1	Italy	41.86064	13.57482	1500	*Fagus sylvatica*	5–10° S	Sedimentary limestone	*Humic Acrisols*	Alpine	01/06/2017
Castelporziano	CPZ1	Italy	41.70423	12.35719	0	*Quercus ilex*	Plain	Volcanic rocks	*Fluvisol*	Mediterranean	26/05/2017
Castelporziano	CPZ2	Italy	41.70429	12.35732	0	*Phillyrea latifolia*	Plain	Volcanic rocks	*Fluvisol*	Mediterranean	26/05/2017
Castelporziano	CPZ3	Italy	41.68068	12.39084	0	*Pinus pinea*	Plain	Volcanic rocks	*Fluvisol*	Mediterranean	26/05/2017
Carrega	EMI1	Italy	44.71998	10.20345	200	*Quercus petraea*	Plain	Alluvial deposits	*Haplic Luvisols*	Continental	14/04/2017
Acquapendente	LAZ1	Italy	42.82746	11.89817	690	*Quercus cerris*	5° WNW	Sedimentary rocks	*Dystric Cambisols*	Mediterranean	01/09/2017
Val Sessera	PIE1	Italy	45.68374	8.06994	1150	*Fagus sylvatica*	30° WNW	Metamorphic rocks	*Haplic Podzols*	Alpine	03/08/2017
Passo Lavazè	TRE1	Italy	46.35825	11.49405	1800	*Picea abies*	10° NNW	Volcanic rocks	*Haplic Podzols*	Alpine	17/06/2017
Pian Cansiglio	VEN1	Italy	46.06335	12.38810	1100	*Fagus sylvatica*	5° E	Limestone	*Haplic Luvisol*	Alpine	26/05/2017
Fundata	FAG	Romania	45.43305	25.26972	1300	*Fagus sylvatica*	20° W	Limestone	*Rendzin*	Alpine	30/03/2017
Mihăești	GORUN	Romania	45.02874	24.99576	500	*Quercus petraea*	10° W	Limestone	*Luvosol*	Continental	07/03/2017
Predeal	MOLID	Romania	45.50694	25.58916	1185	*Picea abies*	20° E	Limestone	*Eutricambosol*	Alpine	01/01/2018
Ștefănești	STEJAR	Romania	44.50567	26.17300	86	*Quercus robur*	Plain	Loess sediments	*Preluvosol*	Continental	30/03/2017

[a] Reference system WGS84.
[b] Classification World Reference Base (WRB) for Soil Resources (FAO, 1998).
[c] Classification according to the EC/92/43 Habitats Directive.

($POD1_{Directive}$, i.e. April to September, 8 to 20 CET), by CLRTAP (2017) ($POD1_{ICP}$, i.e. all year round for Mediterranean evergreen species or April to September for the other forest types, hours with >50 W/m^2 solar radiation), using the SGS/EGS dates estimated within MOTTLES ($POD1_{MOTTLES}$, actual SGS/EGS, hours with >50 W/m^2 solar radiation) or until the time of the visible foliar O_3 injury survey ($POD1_{Survey}$, from SGS to the survey, hours with >50 W m^{-2} solar radiation).

2.2.2.1. Parameterization of the species–specific stomatal ozone flux at the ozone FACE. Stomatal conductance modelling is essential for the estimation of POD_Y (CLRTAP, 2017; Hoshika et al., 2018a). For each dominant target species listed in Table 1, we used the available parameterization in CLRTAP (2017) (Table 3). For *Larix* the parameterization was achieved through literature data of stomatal conductance (Hoshika et al., 2018b) and an unpublished dataset (Agathokleous, pers. comm.). For two species that were not available in the literature, namely *Alnus glutinosa* and *Phillyrea* sp., we measured diurnal courses of stomatal conductance using a portable infra–red gas analyzer (CIRAS–2 PPSystems, Herts, UK) from June to October 2018. The measurements were carried out on potted plants at a Free–Air Controlled Exposure (ozone FACE) facility located at Sesto Fiorentino, in central Italy (43°48′59″N, 11°12′01″E, 55 m a.s.l.). A description of the ozone FACE is available in Paoletti et al. (2017). Leaves with leaf order of 4–8 from the tip of a shoot, which had a healthy appearance, were measured. The estimation of stomatal parameters in response to environmental stimuli was carried out by a standard boundary line analysis as detailed by Alonso et al. (2008) and Hoshika et al. (2012a,b, 2018a, b)).

2.2.2.2. Plant phenology. Phenology for the MOTTLES and Survey accumulation periods was directly assessed at the Romanian sites by following the ICP Forests manual (Beuker et al., 2016). At the French and Italian sites, when no direct observation was carried out, we computed SGS and EGS by using a latitude model according to CLRTAP (2017): with this model, the SGS occurs at DOY 105 at latitude 50°N and it is altered by 1.5 days per degree latitude earlier on moving southward and later on moving northward. Similarly, the EGS is estimated as occurring at DOY 297 at latitude 50°N and is altered by 2 days per degree latitude earlier on moving northward and later on moving southward. In addition, this model considers also the effect of elevation on phenology by assuming a later SGS and earlier EGS by 10 days for every 1000 m a.s.l.

Table 2
Meteorological parameters (mean, minimum and maximum air temperature, solar radiation, vapor pressure deficit (VPD) and soil water content (SWC)) of the forest sites included in the MOTTLES network, averaged over the MOTTLES accumulation period (8–20 CET for simplicity and the growing season of the dominant tree species at each site).

Site	Mean temp, °C	Min temp, °C	Max temp, °C	Solar radiation, W m^{-2}	VPD, kPa	SWC, m^3 m^{-3}
LCAS	15.29	−2.60	27.70	424.80	0.92	NA
MNTFR	16.35	−0.70	30.40	310.23	0.73	NA
MORV	15.65	−0.80	30.50	339.36	0.53	NA
REV	17.47	2.10	33.10	303.38	0.70	NA
ABR1	15.37	0.32	30.24	406.72	0.80	0.20
CPZ1	21.00	−1.28	34.31	353.21	0.93	0.12
CPZ2	21.00	−1.28	34.31	353.21	0.93	0.12
CPZ3	21.00	−1.28	34.31	353.21	0.93	0.17
EMI1	19.72	1.70	34.81	361.96	1.32	0.07
LAZ1	20.17	2.22	37.63	405.70	1.28	0.15
PIE1	12.25	3.00	24.04	284.24	0.47	0.29
TRE1	14.01	−1.80	26.50	361.60	0.73	0.26
VEN1	16.52	1.68	28.43	358.83	0.53	0.38
FAG	12.74	−6.90	27.70	339.18	0.46	0.36
GORUN	18.35	−3.90	36.20	373.70	0.97	0.18
MOLID	15.14	−4.90	30.90	285.48	0.67	0.22
STEJAR	21.11	−2.10	38.90	378.03	1.26	NA

NA, not available over the 2017 accumulation period.

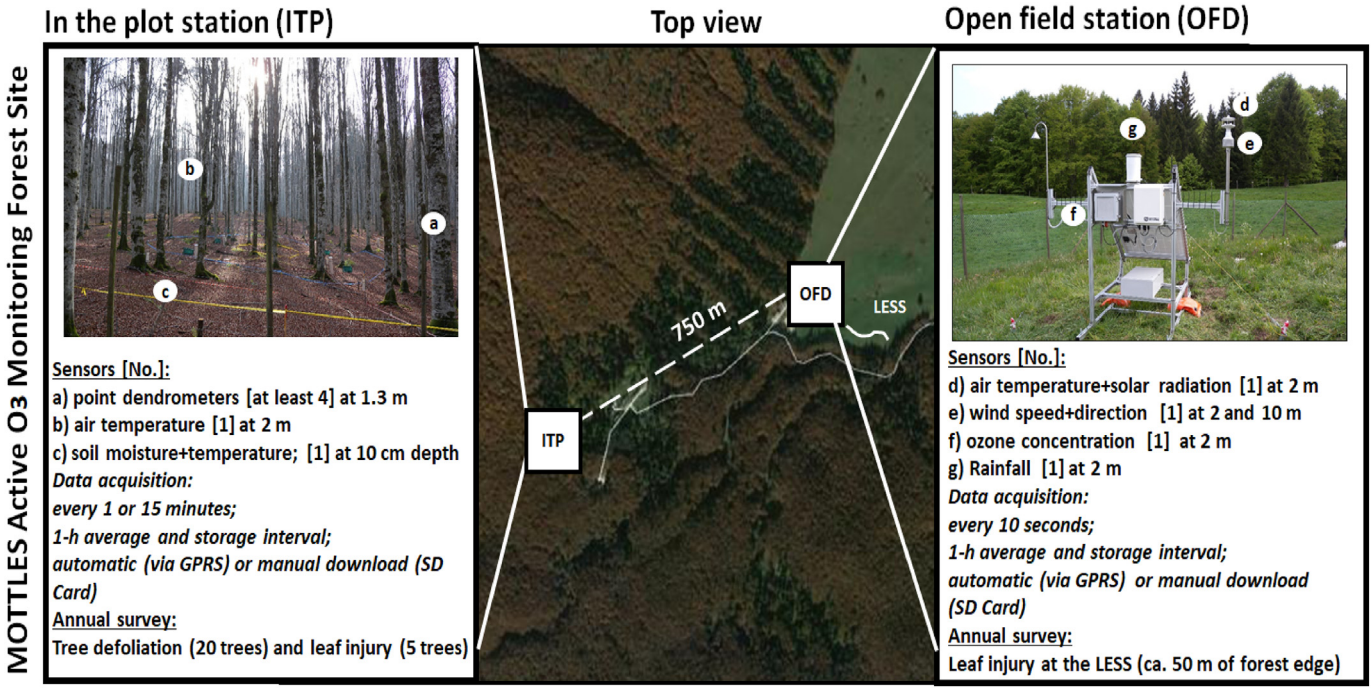

Fig. 2. Description of a typical MOTTLES monitoring station (i.e. VEN1), where two stations (in the plot–ITP and open field–OFD) are coupled with a LESS (Light Exposed Sampling Site). Measures, sensors and acquisition times are shown on left (ITP) and right (OFD).

2.3. Collection of forest–health indicators

The field protocols for the assessment of crown defoliation and visible foliar O_3 injury by MOTTLES surveyors followed the ICP Forests methodologies (Eichhorn et al., 2016; Schaub et al., 2016), slightly adapted to the MOTTLES specific conditions, as explained below. Surveys were carried out by the same two people in each country from August to early–mid September, i.e. the time where O_3 symptoms are more likely to be observed in the MOTTLES countries (Tagliaferro et al., 2005; Schaub et al., 2010). In the case of the French site LCAS, the survey was anticipated to late July because of a prolonged dry period and the risk of early leaf shedding. Annual inter–comparison exercises of the different survey teams were carried out by using the ICP Forests methodologies (Schaub et al., 2016).

2.3.1. Visible foliar ozone injury

At each site, the assessment of visible foliar O_3 injury is conducted every year both within the ITP and along the Light Exposed Sampling Site (LESS). The evaluation of visible foliar O_3 injury is performed on the same five trees in the ITP each year. Required characteristics are: i) crown defoliation must be assessable, ii) no competition among trees, and iii) at least part of the crown must be light exposed. Overall, 85 trees were monitored in the 17 ITPs in 2017. On each tree, five branches of the sun–exposed upper part of the crown were removed and observed immediately by the two surveyors. If sampling was not possible in the ITP, individual trees of the dominant species were selected from the LESS. For deciduous species (incl. broadleaf species and *Larix decidua*), current year (C) leaves/needles were assessed. For evergreen species (incl. Other conifers and *Quercus ilex*), C, one–year–

Table 3
Summary of DO3SE model parameters for the dominant species at each MOTTES site. G_{max}, maximum stomatal conductance; f_{min} minimum stomatal conductance; f_{light_a} parameter determining the shape of the hyperbolic relationship of stomatal response to light (f_{light}, [dl] = dimensionless); T_{max}, T_{opt} and T_{min} are maximum, optimal and minimum temperature for calculating the function f_{temp} that expresses the variation of G_{max} with temperature; VPD_{min} and VPD_{max} are the vapor pressure deficit for attaining minimum and full stomatal aperture (f_{VPD}); SWC_{max} is the soil field capacity and SWC_{min} is the wilting point modelled according with Anav et al. (2016). SGS and EGS are the day of the year (DOY) for start and end of the ozone accumulation period. They are used for calculating the phenological responses of G_{max} (f_{phen}).

Site	Gmax,	f_{min},	f_{light_a},	T_{min},	T_{opt},	T_{max},	VPD_{max},	VPD_{min},	SWC_{max}	SWC_{min}	SGS	EGS
	mmol m^{-2} s^{-1}	fraction	[dl]	°C	°C	°C	kPa	kPa	m^3 m^{-3}	m^3 m^{-3}	DOY	DOY
LCAS	140	0.10	0.0050	0	22	35	0.8	3.5	0.465	0.103	116	289
MNTFR	180	0.10	0.0060	0	20	36	0.6	2.8	0.439	0.066	107	297
MORV	300	0.13	0.0024	5	29	40	1.8	5.7	0.439	0.066	107	297
REV	130	0.16	0.0100	0	14	35	0.5	3.0	0.465	0.103	109	293
ABR1	145	0.02	0.0060	4	21	37	1.0	4.0	0.439	0.066	108	298
CPZ1	195	0.02	0.0120	1	23	39	2.2	4.0	0.439	0.066	1	365
CPZ2	150	0.01	0.0016	0	23	40	1.2	5.3	0.404	0.067	1	365
CPZ3	130	0.03	0.0032	6	20	39	0.6	4.2	0.439	0.066	1	365
EMI1	265	0.13	0.0060	0	22	35	1.1	3.1	0.434	0.047	100	305
LAZ1	265	0.13	0.0060	0	22	35	1.1	3.1	0.465	0.103	102	304
PIE1	145	0.02	0.0060	4	21	37	1.0	4.0	0.439	0.066	111	293
TRE1	130	0.16	0.0100	0	14	35	0.5	3.0	0.434	0.047	117	287
VEN1	145	0.02	0.0060	4	21	37	1.0	4.0	0.465	0.103	110	294
FAG	145	0.02	0.0060	4	21	37	1.0	4.0	0.434	0.047	105	303
GORUN	265	0.13	0.0060	0	22	35	1.1	3.1	0.434	0.047	100	324
MOLID	130	0.16	0.0100	0	14	35	0.5	3.0	0.439	0.066	110	295
STEJAR	200	0.03	0.0035	0	22	50	0.8	7.0	0.434	0.047	94	305

old (C + 1) and two–year–old (C + 2) leaves/needles were assessed, and the three classes were recorded separately. On each leaf/needle, the extent of visible foliar O_3 injury (as a percentage of the total leaf area) was visually scored by using the real percentage, not classes, and results were then averaged for the five branches, resulting in one value per tree. Injury was characterized by small yellow patches or chlorotic mottles (mottling), a reddish–bronze coloration (bronzing) or discoloration of the foliage (photo–bleaching). Leaves or needles with O_3 injury were photographed and crosschecked with existing databases (e.g. Sanz and Calatayud (2018) www.ozoneinjury.org, WSL http://www.ozone.wsl.ch/index-en.ehtml). When it was unclear whether injury was due to O_3, leaf samples were collected for microscopic analyses according to Günthardt-Goerg and Vollenweider (2007). If injury was due to another cause, the sample was excluded from the scoring.

LESS is the light–exposed forest edge closest to the OFD station (maximum radius of 500 m, according to Schaub et al., 2016). The length of the LESS was ca. 50 m and the width was 1 m. The number of possible non–overlapping quadrates was determined according to the adjusted sample size (10% error) and their position along the LESS was randomly chosen. Presence or absence of visible foliar O_3 injury was estimated for the vegetation in each quadrate, at the same period as for the vegetation in ITP. Visible injury in the LESS was photographed and sampled in order to be preserved in a herbarium. The species classification followed Flora Europaea (Tutin et al., 1993).

In case foliar O_3 injury occurred in a species not present in the literature, validation was carried out by the ozone FACE. In 2017, only *Sorbus aucuparia* and *Vaccinium myrtillus* needed a validation. Potted plants were exposed to three levels of O_3, similarly to the protocol in Hoshika et al. (2018a): ambient air (AA), 1.5 times ambient O_3 concentration (1.5 × AA), and 2.0 times ambient O_3 concentration (2.0 × AA). Hourly mean O_3 concentrations during the experimental period (1 May to 31 October 2018) were 35.2 ppb in AA, 53.1 ppb in 1.5 × AA and 65.2 ppb in 2.0 × AA. AOT40 values in AA, 1.5 × AA and 2.0 × AA were 22.8 ppm·h, 60.2 ppm·h and 92.6 ppm·h, respectively, during the experimental period. Plants were irrigated to field capacity every 2–3 days to avoid water stress. All attached leaves were evaluated every week by the same two well–experienced observers. Pest, pathogen and mechanical injury was not considered. Injury was characterized both qualitatively (by collecting samples for microscopy analysis) and quantitatively (by quantifying the extent as a percentage of the total leaf area).

2.3.2. Crown defoliation

Defoliation, estimated visually, expresses loss of leaves/needles in the crown of a tree compared to a reference tree of the same species, with full foliage, in the immediate vicinity of the sample site or a photo image applicable to a tree species (Badea, 2008). The assessable crown includes only those parts that are not influenced by other crowns i.e. by shading (Fig. 1S). For ICP Forests, crown condition assessments are mandatory at least once a year (Eichhorn et al., 2016). The time of the assessment should be between the end of the first flush of foliage (when leaves and needles are fully developed) and the beginning of autumnal senescence. For most species, the most suitable time for the assessment is from mid–July until end of August. The assessments must be done during the same period and under similar conditions each year. In regions with scarce water availability or subjected to severe drought which may damage plants (Granier et al., 2007), the assessment may be shifted to early summer.

Within each MOTTLES site, 20 predominant, dominant and codominant trees (Kraft classes I–III) were selected for crown assessment. Surveys were carried out at the same time as the visible injury surveys. The intensity of each type of defoliation (Table 1S) was recorded by 5% steps (ex. 0, 5, 10, 15 … 100%) according to the ICP Forests protocol (Eichhorn et al., 2016). Defoliation related to biotic and anthropic reasons or fire was not included in our analyses.

2.3.3. Radial growth

Variations in stem radius were continuously monitored by automatic point dendrometers on a minimum of 4 trees per site, selected from the 20 trees used for assessing crown defoliation. We used linear variable transducers (RS Pro LM10 Series, Rs Component s.r.l.) that measure the linear displacement of a stainless–steel sensing rod (effective travel 10 ± 0.5 mm, linear thermal expansion coefficient 2.5 × 10^{-6} K^{-1}), which is pressed against the bark. The transducer was mounted on a frame attached to the stem by two titanium rods at 130 cm above the ground (breast height). As the stem expands or contracts, the rod transmits the signal to the transducer. The sensor output, V1/Vx ratio, was converted into a numerical value (length of sensor in millimeters) using a linear calibration regression equation (Giovannelli et al., 2007). Raw data were averaged every hour. Daily dendrometer data were used to estimate seasonal stem radial growth. The sum of daily increments of the stem was interpolated by a modelling approach using a Gompertz function and fitted by nonlinear regression to estimate the pattern of intra–annual secondary growth. The Gompertz function fitted between the sum ΔR (sum and time DOY) was:

$$y = \mathrm{Aexp}\left[-\exp^{(\beta-\kappa t)}\right] \quad (5)$$

where A, β, κ, t were the parameters of the function representing growth asymptote, x–axis placement parameter, the rate of change of the curve and time (expressed as day of the year), respectively. The difference between upper asymptote and lower asymptote (A) defined the annual stem radial growth.

2.4. Data analysis

Linear correlations between AOT40 and POD1 were calculated over different accumulation windows, as well as among forest–health indicators and O_3 metrics, and tested for significance at $p < .05$ by using Statistica 10.0 package. Normal distribution was tested by Lilliefors (Kolmogorov–Smirnov) test. As visible foliar injury and radial growth were not normal, the non–parametric Spearman correlation test was applied. Only input values (i.e. metrics) calculated on >75% of the O_3 hourly data were included in this correlation analysis.

3. Results and discussion

3.1. Network set-up

One of the major decisions while planning the network set-up was establishing the right depth of the SWC sensors. The estimated depth at which 50% of total root is accumulated for different temperate agricultural crops varies from 8 cm to 20 cm (Fan et al., 2016). In a forest, deeper rooting is common, even though most of the absorbing fine roots are in the upper soil profile in the top 30 cm of soil (Jackson et al., 1996; Rytter and Hansson, 1996; Schenk and Jackson, 2002; Finér et al., 2011). The phenomenon of hydraulic lift – i.e. water absorbed by deep roots moves upwards through the roots, is released in the upper soil profile at night and is stored there until it is resorbed by roots the following day – is also very common for forest trees (Caldwell et al., 1998; Gaines et al., 2015). We thus postulated that a sensor placed in the middle of the upper 0–20 cm layer was representative of the effects of soil availability to the roots and the stomata. For instance, Anav et al. (2018) compared no soil water limitation to stomatal conductance with a shallow rooting zone (i.e. SWC at 10 cm) and showed that the difference in O_3 dry deposition can be up to 90%. However, a comparison with the results recorded at different depths (10, 30, 60 cm) at few sites (ABR1, LAZ1, TRE1) is in progress, and will allow verifying whether this assumption is correct.

Monitoring of O_3 and other environmental variables started in March–June at 14 out of the 17 sites (Table 1). Two Italian stations started in August–September. The percentage of available hourly O_3 data depended on the accumulation window (Table 1); for some sites it was <75% and thus not sufficient for this analysis. One station in Romania got a major failure with the O_3 monitor and thus was not included in this work. For the other environmental variables, in occasional cases of missing data caused by the temporary failure of a sensor, the following functions were used in accordance with Anav et al. (2016): $f_{temp} = 0.75$ (temperature), $f_{light} = 0.75$ (solar radiation), $f_{VPD} = 1$ (vapor pressure deficit), $f_{SWC} = 1$ (soil water content). The SWC sensors were installed at the French stations only in September and thus the calculation of POD1 assumed $f_{SWC} = 1$ for these sites.

Visits for technical maintenance were needed (on average, three times a year), mostly for replacement of the O_3 monitor filters, calibration or replacing parts of sensors, solving problems of data transmission and power supply.

3.2. Ozone metrics

The highest day-time O_3 average during the recording period (55 ppb) was measured at an Italian site in central Italy (ABR1), followed by a site in southern France (48 ppb, LCAS) (Table 4). The lowest concentrations were observed in Romania, with average values of 21 ppb at STEJAR and GORUN. The average of all MOTTLES sites was 38 ppb. Such values are in the range measured by traditional monitoring stations at remote sites in these countries. For instance, the day-time average recorded in France over the time period 1999–2012, resulting from 61 rural stations, was 34 ppb (Sicard et al., 2016b). A direct monitoring of O_3 concentrations at forest sites is important because the values recorded at traditional monitoring stations may be still affected by traffic–emitted NOx thus showing a degradation of O_3 by NO (Sicard et al., 2013). In contrast, very high hourly concentrations may occur at both forest and remote sites, as also found by Paoletti et al. (2014). For instance, the highest 1-h spike was recorded at ABR1 (140 ppb), while the average of all MOTTLES sites was 90 ppb. The maximum peak was 169 ppb at 14 Italian rural stations in 2000–2004 (Paoletti, 2006) and exceeded 100 ppb and 120 ppb over the time period 2000–2010 in southern France – central Italy and northern Italy, respectively (Sicard et al., 2013).

The average $AOT40_{Directive}$ calculated for sites with at least 75% of hourly data, was 14,964 ppb h and thus almost three times the EC legislative standard established at 5000 ppb h. The highest $AOT40_{Directive}$ value was in Italy (43,702 ppb h at EMI1) and the lowest values were in Romania (<3000 ppb h at STEJAR and GORUN). When AOT40 was accumulated over the time period recommended by ICP Vegetation ($AOT40_{ICP}$), values were similar to $AOT40_{Directive}$ values (on average + 1.5%), and even higher when we used the MOTTLES accumulation window (on average + 19%). This is not surprising because the accumulation windows are 183 days for $AOT40_{Directive}$ as well for $AOT40_{ICP}$, and from 168 days to 210 days (depending on the tree species) for $AOT40_{MOTTLES}$. We recorded the lowest average value as $AOT40_{Survey}$ (12,369 ppb h), where the accumulation period is the shortest one since surveys were realized before the end of the growing season.

The highest POD1 values were at French sites (31–39 mmol m^{-2} $POD1_{Directive/ICP}$), where the SWC sensors were installed at the end of the growing season and thus POD1 was calculated assuming no SWC limitation ($f_{SWC} = 1$). This result stresses the critical role of SWC in affecting the stomatal uptake of O_3 and thus the need of including f_{SWC} in the POD_Y calculation (De Marco et al., 2016; Anav et al., 2018). The Romanian sites showed $POD1_{ICP}$ values as high as 13–25 mmol m^{-2}, although f_{SWC} was included in the POD1 estimation. Such high values in Romania are mostly due to the temperate continental climate which is not limiting stomatal uptake as strong as in Italy (De Marco et al., 2017). POD1 values accumulated over the time window recommended by the EC Directive and ICP are exactly the same for the considered sites, since there are no evergreen Mediterranean species. Those values on average were 20% and 35% higher relative to $POD1_{MOTTLES}$ and $POD1_{survey}$, respectively.

A good agreement was found between our POD estimates and the POD data available in the literature. Modelling studies estimated POD1 values to be 2–30 mmol m^{-2} in Southern Europe (Anav et al., 2016; Sicard et al., 2016a). In field conditions in Italy, POD1 values were reported to be around 28–50 mmol m^{-2} for poplars (Hoshika et al., 2018b; Zhang et al., 2018) and 4–19 mmol m^{-2} for oaks (Hoshika et al., 2018a).

Previous experimental studies have investigated the stomatal-flux based CLs above which O_3 injury could occur (CLRTAP, 2017). To the best of our knowledge, the CLs for alder (in MORV), larch (in LCAS) and *Phillyrea* (in CPZ2) have not been investigated yet. However, 90% of the sites (i.e. 86% of the sites where the SWC effect was considered in the POD1 calculation) showed POD1 values exceeding the CLs corresponding to a 5% biomass reduction. Such CLs were calculated under open–air experimental conditions (POD1 = 5.0 to 8.8 mmol m^{-2} for oaks in Hoshika et al., 2018a; POD1 = 5.1 mmol m^{-2} for poplars in Zhang et al., 2018) and open–top chamber experiments (POD1 =

Table 4
Average (avg ± standard deviation) and minimum (min)–maximum (max) hourly ozone concentration over the total number of days of recording (DR) and day-time hours; percentage of available hourly data (ahd) according with the different calculation approaches (Directive, ICP, MOTTLES and Survey) and respective AOT40 and POD1 in the year 2017.

Code	Ozone concentration (day-time hours)			ahd, %				AOT40, ppb h				POD1, mmol m^{-2}			
	avg, ppb	Min–max, ppb	DR, No	Directive	ICP	MOTTLES	Survey	Directive	ICP	MOTTLES	Survey	Directive	ICP	MOTTLES	Survey
LCAS**	47.6 ± 7.9	13–70	198	97.19	93.64	93.23	99.65	24,207	23,828	19,829	14,264	31.29	31.29	29.40	18.40
MNTFR**	37.9 ± 9.2	10–72	274	98.01	98.31	98.43	98.50	9203	9406	8134	6583	35.48	35.48	34.16	21.29
MORV**	32.5 ± 12.7	0–72	206	100	100	100	100	8592	8802	8813	6947	38.82	38.82	27.48	25.87
REV**	30.8 ± 11.3	0–99	285	99.28	99.31	99.17	99.42	7145	7490	6611	6073	25.28	25.28	23.25	15.04
ABR1	55.2 ± 17.6	0–140	146	66.30	67.64	76.62	69.75	*	*	44,045	*	*	*	12.74	*
CPZ1**	34.1 ± 19.3	1–91	219	72.83	60.16	56.48	42.25	*	*	*	*	*	*	*	*
CPZ2**	34.1 ± 19.3	1–91	219	72.83	60.16	56.48	42.25	*	*	*	*	*	*	*	*
CPZ3	34.1 ± 19.3	1–91	219	72.83	60.16	56.38	42.15	*	*	*	*	*	*	*	*
EMI1	45.9 ± 20.8	4–105	196	99.64	92.04	94.75	96.00	43,702	42,344	43,706	36,234	8.93	8.93	0.61	7.43
LAZ1	43.3 ± 8.7	18–68	60	0	14.38	26.20	1.25	NA	*	*	*	NA	*	*	*
PIE1	45.7 ± 11.8	14–97	78	0	28.62	38.08	15.27	NA	*	*	*	NA	*	*	*
TRE1	45.3 ± 10.3	16–100	197	48.91	57.69	69.45	59.06	*	*	*	*	*	*	*	*
VEN1	34.0 ± 15.9	3–102	148	74.0	73.55	83.71	78.02	*	*	19,322	17,107	*	*	22.71	24.26
FAG	43.1 ± 8.9	21–75	205	100	100	100	100	12,658	13,424	13,581	12,484	24.93	24.93	26.72	22.99
GORUN	21.3 ± 15.8	0–72	236	97.92	99.87	92.52	100	7716	7613	7797	6806	13.12	13.12	9.82	11.92
MOLID	NA	NA	0	0	0	0	0	NA	NA	NA	NA	NA	NA	NA	NA
STEJAR	21.4 ± 15.7	0–101	220	100	100	99.92	100	6488	5012	5033	4829	22.89	22.89	23.81	20.51

*Percentage of hourly data <75%; **POD0 estimated with a standard value of soil moisture ($f_{SWC} = 1$); NA = data not recorded.

6.3 mmol m^{-2} for beech and birch, POD1 = 23.8 mmol m^{-2} for needle leaf trees, and POD1 = 26.3 mmol m^{-2} for Aleppo pine, holm oak and Norway spruce in Büker et al., 2015).

Generally, we found a good agreement between values of the same metric accumulated over different time windows (Fig. 3). Similar results were obtained in a correlation of 34 exposure–based O_3 metrics (Paoletti et al., 2007). This is an important finding because it suggests that the metrics used for the protection of forests in Europe (Directive, ICP) are representative of the accumulated concentration or flux based exposure as measured in our network, both over the entire growing season (MOTTLES) and over the period from the SGS to the time that field injury was surveyed (Survey).

In contrast, the agreement between AOT40 and POD1 values was poor, because at most sites high values of AOT40 corresponded to low POD1 values and *vice–versa* (Fig. 3). Such negative correlation suggests that the environmental conditions favouring elevated O_3 concentrations and thus high AOT40, also lead to a stomatal closure and hence low POD1. In other words, the conditions stimulating stomatal O_3 uptake did not occur at the time of elevated O_3 pollution. Discrepancies in the spatial and temporal distribution of AOT40 and POD have been frequently highlighted in the literature (Simpson et al., 2007; Mills et al., 2011; De Marco et al., 2015; Anav et al., 2016) and suggest that the exposure–based metric AOT40 may provide misleading results when used for the protection of forests from O_3 (Anav et al., 2019).

3.3. Visible foliar ozone injury

Visible foliar O_3 injury is considered as an important forest–health indicator in forest monitoring (Schaub et al., 2016; Sicard et al., 2016a) because it is specific of O_3 injury and is not caused by other co–occurring factors (Günthardt-Goerg and Vollenweider, 2007; Schaub et al., 2010). Ozone levels at 12 of our 17 sites were high enough to negatively affect trees by inducing typical visible foliar O_3 injury in the ITP and/or in the LESS (Table 5).

The highest percentages of visible foliar O_3 injury in the dominant ITP species were observed in *Pinus sylvestris* (MNTFR). *Fagus sylvatica*

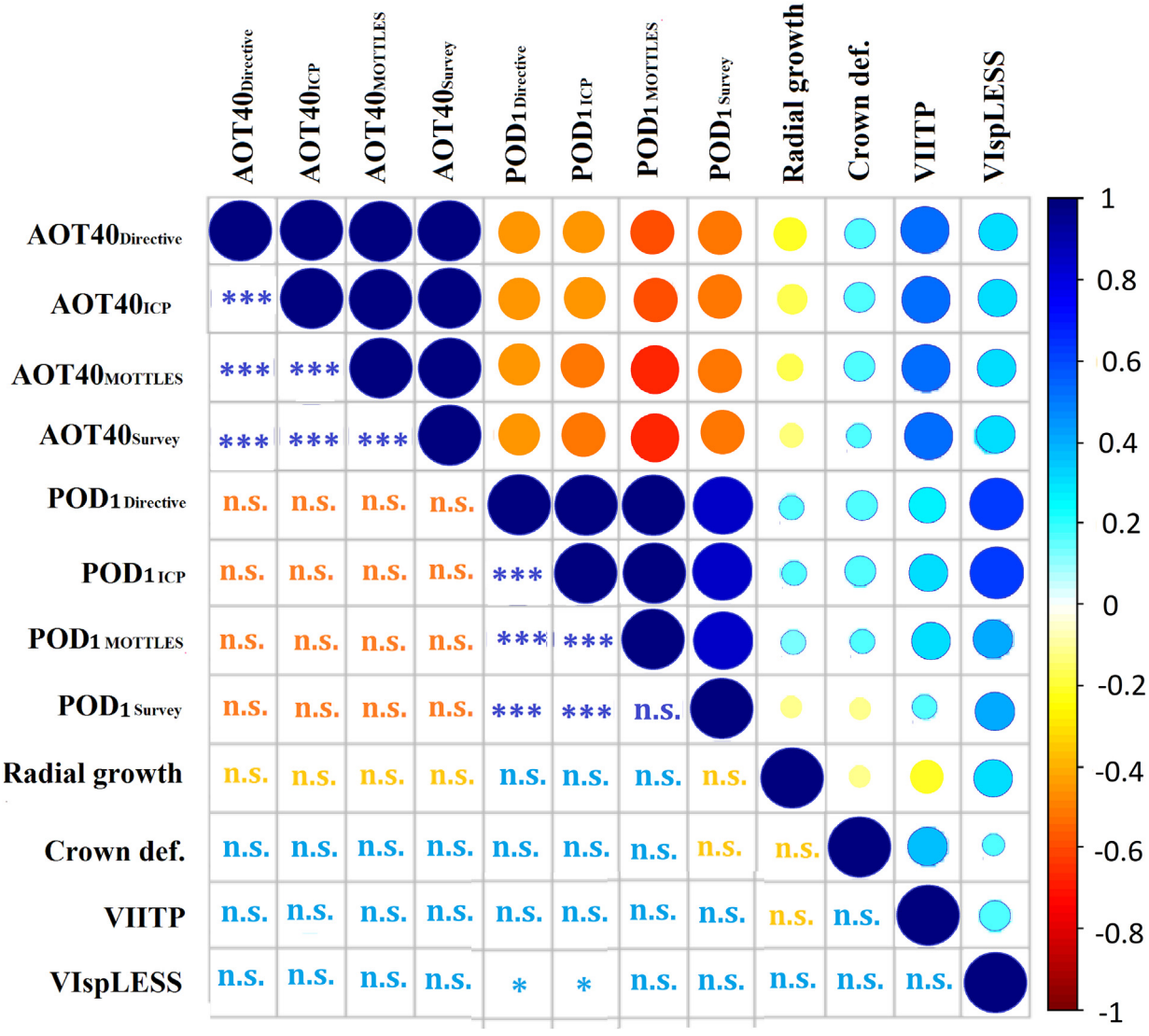

Fig. 3. Relationship between AOT40, POD1 and forest–health indicators. AOT40 and POD1 are calculated according to the European Directive (Directive, i.e. April to September, 8 to 20 CET), CLRTAP (2017) (ICP, i.e. all year round for Mediterranean evergreen species or April to September for the other forest types, hours with >50 W/m^2 solar radiation), the start and end of the growing season estimated within MOTTLES (MOTTLES, actual SGS/EGS, hours with >50 W/m^2 solar radiation) or until the time of the visible injury survey (sur, from SGS to the survey, hours with >50 W/m^2 solar radiation). Forest–health indicators are tree radial growth, crown defoliation (Crown def.), visible foliar ozone injury estimated on the dominant tree species in the plot (VI ITP) and percentage of symptomatic species in the LESS (VIsp LESS). Only accumulation windows with >75% hourly data were included. Positive correlations are displayed in blue and negative correlations in orange. Colour intensity and size of the circle are proportional to the correlation coefficient; empty cells indicate correlation = 0; *p < .05, **p < .01, ***p < .001, n.s. = not significant.

showed O_3 injury at two ITP sites in Italy (PIE1 and VEN1). French plots of *Picea abies* (REV), *Alnus glutinosa* (MORV) and *Larix decidua* (LCAS) also recorded high percentages of visible foliar O_3 injury. However, other two sites with *P. abies* (TRE1 and MOLID), all the sites with oaks and all the sites in Romania did not show foliar injury in the dominant ITP species. Relative to the POD1 values calculated according to the Directive, ICP and MOTTLES accumulation periods, visible foliar O_3 injury were found in ITPs of sites that exceeded the CLs estimated by Sicard et al. (2016a) for conifers (24 mmol m^{-2}) and broadleaves (20 mmol m^{-2}).

In French (MNTFR; LCAS), Italian (VEN1; LAZ1) and Romanian (GORUN) LESS areas, visible foliar O_3 injuries were identified in *F. sylvatica*, *Prunus* species and brambles (*Rubus ulmifolius* and *R. fruticosus*). In many French LESS areas, injured individuals were observed in species known to be sensitive to O_3, such as *Corylus avellana*, *Carpinus betulus*, *Viburnum opulus*, *Sorbus aria* and *Fraxinus excelsior*. Two species of sorb (*Sorbus aria* and *S. aucuparia*) were O_3–injured in France, Italy and Romania. Furthermore, alder (*A. glutinosa*) and spruce (*P. abies*) showed O_3 injury similarly to what was recorded for the dominant ITP species. By comparing those data with POD1, visible foliar O_3 injury in the LESS occurred at sites with POD1 slightly lower than the CLs suggested for deciduous species (Sicard et al., 2016a): *F. sylvatica* in ABR1 and GORUN, as well *R. ulmifolius* in EMI1 were injured despite a POD1 <20 mmol m^{-2} (Tables 4, 5).

When investigating which O_3 metric was better correlated with visible foliar O_3 injury, we did not find any significant correlation in the ITP (Fig. 3). This does not necessarily mean a lower injury inside the forest, while it was possibly a statistical artifact due to the limited time period investigated so far (only the year 2017) and the limited sampling of leaves relative to the large size of those adult trees (on average 29.9 cm as breast–height diameter, Table 5). Sampling five random branches was often unable to detect any injury in these large crowns, even though there was plenty of injury in the LESS. In fact, the percentage of injured species in the LESS (19% per site on average) showed a positive and significant ($p < .001$) correlation with $POD1_{Directive}$ and $POD1_{ICP}$ ($r = 0.72$; Fig. 3). This can be explained with the following main reasons: a) it is well known that young trees, more frequent at forest edges, are more sensitive to ozone injury compared with adult trees (Nunn et al., 2005); b) visible foliar O_3 injury is more easily found on basal leaves when exposed to light (Yuan et al., 2016); c) the high number of species present in the LESS increases the possibility of sampling O_3-sensitive species. We thus conclude that monitoring visible foliar O_3 injury in the LESS is a better approach than recording the same injury in the ITP. In addition, the former approach is also easier and less time–consuming than the latter.

As a confirmation that AOT40 is not an optimal metric for forest protection from O_3, visible foliar O_3 injury was not significantly correlated with AOT40 (Fig. 3). The better performance of POD1 in explaining visible foliar O_3 injury of forests than AOT40 confirms previous results by Sicard et al. (2016a) and Araminiene et al. (2019) even though the metrics in these papers were modelled and not calculated on the basis of direct *in–situ* measurements, as we made in the MOTTLES network.

3.4. Crown defoliation

The MOTTLES network showed a large variability also in terms of crown conditions. The average crown defoliation of all Romanian sites, one site in Italy (EMI1) and two sites in France (MORV and REV) was ≤10% (Table 5), i.e. the trees may be considered as healthy, according to the crown defoliation classification by UN/ECE – ICP Forests (2010). Seven sites were in Class 1 defoliation (11–25%), and the remaining sites (all in Italy) were in Class 2 defoliation (26–60%).

Crown defoliation is an aspecific forest–health indicator of injury because it responds to different biotic and abiotic factors, including climatic conditions, pests, site characteristics, air pollution (Sicard et al., 2016a). In fact crown defoliation was not significantly correlated with

Table 5
Assessment of plant–response indicators at MOTTLES sites in 2017. Mean tree diameter and annual radial growth of the dominant species (±SD); day of the year (DOY) of the survey; crown defoliation (mean score of tree crowns per plot) and visible foliar ozone injury (mean percentage of injured leaf/needle surface averaged for branches, trees and plot) of current year foliage (C) when the dominant ITP (in the plot) species is deciduous, and C, C + 1 and C + 2 for evergreen species; type and percentage of injured species (e.g. number of species with visible foliar ozone injury divided for the total number of species detected) in the LESS (Light Exposed Sampling Site). For a description of ITP and LESS, see Fig. 2.

Site	Tree diam., cm	Radial growth, mm	DOY	In the ITP		In the LESS	
				Crown Defol, %	Leaf injury, %	Injured species	Injured species, %
LCAS	30.3 ± 2.2	NA[b]	207	13.2 ± 6.9	9.6 ± 5.2 (C)	*Acer pseudoplatanus*, *Angelica archangelica*, *Prunus avium*, *Prunus* sp., *Rosa canina*, *Rubus fructicosus*, *Sorbus aria*, *Verbascum thapsus*	33.3
MNTFR	38.2 ± 3.2	NA	213	18.2 ± 7.2	0 (C) 15.8 ± 3.6 (C + 1) 25.2 ± 5.8 (C + 2)	*Fagus sylvatica*, *Picea abies*, *Quercus robur*, *Rubus fructicosus*	12.5
MORV	23.1 ± 21.2	NA	214	7.8 ± 3.4	4.6 ± 2.4 (C)	*Carpinus betulus*, *Corylus avellana*, *Viburnum opalus*	50.0
REV	35.1 ± 31.6	NA	215	10.0 ± 5.1	0 (C) 3.0 ± 2.1 (C + 1) 8.2 ± 2.3 (C + 2)	*Acer pseudoplatanus*, *Alnus glutinosa*, *Corylus avellana*	42.9
ABR1	49.0 ± 6.6	0.68 ± 0.37	244	28.2 ± 7.8	0 (C)	*Fagus sylvatica*, *Rubus idaeus*, *Sorbus aucuparia*[a]	43.0
CPZ1	42.8 ± 19.1	0.11 ± 0.13	242	26.2 ± 8.6	0 (C)	No species	0
CPZ2	8.9 ± 0.9	0.31 ± 0.10	242	38.0 ± 18.9	C 0	No species	0
CPZ3	47.8 ± 10.5	NA	242	35.0 ± 9.3	0 (C) 0 (C + 1) 0 (C + 2)	No species	0
EMI1	28.07 ± 1.2	0.70 ± 0.26	234	10.0 ± 17.0	0 (C)	*Rubus ulmifolius*	9.1
LAZ1	29.8 ± 6.8	1.01 ± 0.52	244	23.8 ± 7.1	0 (C)	*Prunus* sp., *Rubus ulmifolius*, *Clematis vitalba*	30.0
PIE1	27.5 ± 6.1	0.11 ± 0.01	235	22.7 ± 15.8	0.8 ± 1.4 (C)	*Fagus sylvatica*, *Corylus avellana*	25.0
TRE1	51.3 ± 9.2	0.53 ± 0.59	236	12.7 ± 9.6	0 (C) 0 (C + 1) 0 (C + 2)	*Vaccinium myrtillus*[a]	20.0
VEN1	49.1 ± 11.2	0.44 ± 0.32	237	21.2 ± 2.2	4.6 ± 2.2 (C)	*Fagus sylvatica*	25.0
FAG	26.6 ± 5.1	2.34 ± 1.09	255	9.5 ± 3.9	0 (C)	*Sorbus aucuparia*	20.0
GORUN	30.8 ± 4.2	1.52 ± 0.60	255	12.8 ± 3.4	0 (C)	*Fagus sylvatica*	6.2
MOLID	52.2 ± 5.9	0.41 ± 0.28	255	11.2 ± 3.2	0 (C)	No species	0
STEJAR	39.8 ± 5.3	0.54 ± 0.21	254	18.2 ± 5.4	0 (C)	*Ulmus minor*	4.2

[a] Under validation at the ozone FACE.
[b] NA = not available due to late start of data recording.

any O_3 metric (Fig. 3). This result contrasts with results from experimental studies (e.g. Hoshika et al., 2013) and would suggest that crown defoliation is not suitable as forest–health indicator for the protection of forests against O_3. These results are similar to those obtained by Sicard et al. (2016a) and Araminiene et al. (2019) by modelling the metrics and relating them to measured crown conditions. In these papers, POD1 did not produce significant correlations, while crown conditions improved with increasing AOT40.

3.5. Radial growth

The stem diameter of the four dominant trees monitored by dendrometers at each site varied according to the species and site (Table 5). Overall, in 2017 the tree diameter ranged from 8.9 ± 0.9 cm of CPZ2 (*Phillyrea latifolia*) to 52.2 ± 5.9 cm of MOLID (*Picea abies*). Although these species–specific differences determined a wide variability, we argue that in temperate environments the intra–annual dynamic of stem growth is very similar resulting in a S–shaped pattern for most of the tree species (Deslauriers et al., 2003; Cocozza et al., 2016; Zweifel et al., 2016). In addition, it is well documented that the sensitivity of trees to environmental constrains is size–dependent (Oberhuber et al., 2014; Balducci et al., 2016). So the wide range of the tree sizes monitored within the MOTTLES network represents a useful approach to study the effect of combined stresses such as warming, drought and O_3 exposure on the intra–annual stem growth.

During the growing season 2017, stem radial growth was recorded in all the trees, suggesting that wood formation occurred in all the monitored trees (except for a *Q. ilex* tree in CPZ1). Because wood formation is very sensitive to abiotic stresses, the cambium activity (i.e. stem growth) represents a powerful proxy of the tree vitality and health (Abe et al., 2003; Traversari et al., 2018). The annual stem radial growth ranged between 2.34 ± 1.09 mm for *F. sylvatica* at FAG to 0.11 ± 0.13 mm at CPZ1 (*Q. ilex*). At Italian sites, *F. sylvatica* growing in ABR1 and VEN1 had higher stem radial growth than in PIE1 (0.68 and 0.44 mm y^{-1} vs 0.11 mm y^{-1}, respectively) while deciduous oaks at EMI1 and LAZ1 showed similar growth rates (0.70 and 1.01 mm y^{-1}, respectively). At Romanian sites, deciduous oaks showed a wide range of growth variation with 1.52 ± 0.6 and 0.54 ± 0.2 mm y^{-1} at GORUN and STAJAR respectively. Our results agree with previous data for the Italian sites and species reported by Bertini et al. (2011). The general low radial increment of beech in the Italian sites ABR1 and VEN1 (when compared to the beech growing in the Romanian site FAG) could be related to the high sensitivity of this species to the recurrent drought and warming events occurring in the last decade at these sites (Bertini et al., 2013). In species with pre–determined growth as beech and oak, the effect of disturbance of the current year can have detrimental effect on the growth rate of the next years (Dobbertin et al., 2006). Similar stem radial growths were recorded in *P. abies* growing in Italian and Romanian sites (0.53 and 0.41 mm y^{-1}, respectively). Previous investigations in the spruce forest TRE1, reported an annual stem diameter increment of 0.8 cm y^{-1} (Fabbio et al., 2008). The low stem radial increment (0.53 mm y^{-1}) recorded by our dendrometers in 2017 confirmed that the TRE1 forest was not productive any more.

The impact of O_3 on radial growth of adult trees has been poorly investigated under field conditions. McLaughlin et al. (2007) observed that ambient O_3 caused a periodic slowdown in seasonal growth patterns that was attributable in part to amplification of diurnal patterns of water loss in the stem of the investigated six trees. In Switzerland, Braun et al. (2017) found a reduction of radial growth in beech and Norway spruce due to stomatal O_3 uptake, which was associated with a reduced mycorrhizal activity. Matyssek et al. (2010) reported that O_3 decreased radial growth at breast height by 11% and stem productivity by 44% in beech after a 8-year free-air exposure to O_3. A recent study on European beech correlating data of National Forest Inventory and O_3 metrics stressed the necessity to have finer time-resolution investigations in order to evaluate the effect of O_3 on forest growth (Paoletti et al., 2018). To our knowledge, MOTTLES is the largest network for continuous monitoring of radial growth of trees under O_3 exposure. On the basis of our data, no significant correlation between radial growth and O_3 metrics in 2017 was found (Fig. 3), possibly because the size of our dataset was still insufficient to account for the many variables affecting radial growth of adult trees. We expect more robust estimates when more years of monitoring will be available.

3.6. Correlations among forest–health indicators

Crown defoliation increased with increasing visible foliar O_3 injury (Fig. 3) suggesting that a tree affected by visible foliar O_3 injury was also more defoliated. In contrast, radial growth decreased with increasing visible foliar O_3 injury i.e. a tree affected by O_3 injury showed a lower annual radial growth. Plants weakened by O_3 may be more susceptible to pests, disease and drought (Krupa et al., 2001), then to crown defoliation and inhibited growth. Further research is clearly warranted to determine the two–way interaction, i.e. cause–effect relationships and contributions of the multiple stress factors to forest health.

4. Conclusions

The network of instrumented forest sites described here is aimed at an epidemiological assessment of POD_Y –based critical levels for the protection of forests from O_3. Results presented here are from the first year of activity; new evaluations will be carried out in the following years as the results in the short term may not converge with those in the long term. Moreover, the growing season data are partly incomplete for few sites because some sensors were installed after the beginning of the 2017 growing season. Such condition could determine a bias toward the second part of the growing season. Overall, we can conclude that: i) our network is representative of a large range of O_3 pollution levels; ii) O_3 pollution is harmful for forest health, because trees showing visible foliar O_3 injury were more defoliated and showed a lower annual radial growth than trees with no visible O_3 injury: the timing of the defoliation assessment is important to realize if crown defoliation is due to damaged leaves dropping off earlier in the season because of O_3; iii) the metrics used for the protection of forests in Europe (Directive, ICP) are well correlated to the metrics calculated on the basis of the real duration of the growing season (MOTTLES) and are thus representative of the actual exposure/flux; iv) AOT40 and POD1 are uncoupled, in that high values of AOT40 often corresponded to low POD1 values and *vice–versa*. As POD is considered a more biologically–meaningful metric, AOT40 cannot be recommended as an optimal metric for forest protection from O_3; v) visible foliar O_3 injury correlates better with POD1 than with crown defoliation and radial growth, and is thus a good forest–health indicator of tree responses to O_3 under field conditions; vi) monitoring visible foliar O_3 injury in the LESS is a better approach than recording the same injury in the ITP. These results are useful to monitoring experts and environmental policy makers.

Given the recent interest in monitoring the impacts of O_3 on forests by assessing the exceedance of POD_Y critical levels and O_3 visible foliar injury as requested by the NEC Directive (De Marco et al., 2019), the MOTTLES approach is a good example of expanding monitoring at existing long-term forest monitoring sites with assessments of stomatal O_3 flux and its relationships with tree biological responses. We wish that our results may stimulate the development of similar networks all over the world, because only monitoring at forest sites is truly representative of the actual stomatal O_3 flux conditions. These measures will also warrant the further improvement and validation of models and their parameterizations.

Acknowledgments

This work was carried out with the contribution of the LIFE financial instrument of the European Union (LIFE15 ENV/IT/000183) in the

framework of the MOTTLES project "Monitoring ozone injury for setting new critical levels" and the technical support by: Écrins National Park, Morvan Regional Natural Park, Electricity of France, Certified Associations of Air Quality Monitoring (Atmosf'air Bourgogne, Atmo Grand–Est, Atmo Auvergne–Rhône–Alpes, Atmo Nouvelle–Aquitaine), the MERA programme, funded by the French Ministry for Ecological and Solidary Transition, Comando Unità Forestali, Ambientali e Agroalimentari Carabinieri (CUFA) and all the Institutions managing the Italian sites.

Appendix A. Supplementary data

Supplementary data to this article can be found online at https://doi.org/10.1016/j.scitotenv.2019.06.525.

References

Abe, H., Nakai, T., Utsumi, Y., Kagawa, A., 2003. Temporal water deficit and wood formation in *Cryptomeria japonica*. Tree Physiol. 23, 859–863. https://doi.org/10.1093/treephys/23.12.859.

Alonso, R., Elvira, S., Sanz, M.J., Gerosa, G., Emberson, L.D., Bermejo, B., Gimeno, B.S., 2008. Sensitivity analysis of a parameterization of the stomatal component of the DO3SE model for *Quercus ilex* to estimate ozone fluxes. Environ. Pollut. 155, 473–480. https://doi.org/10.1016/j.envpol.2008.01.032.

Anav, A., De Marco, A., Proietti, C., Alessandri, A., Dell'Aquila, A., Cionni, I., Friedlingstein, P., Khvorostyanov, D., Menut, L., Paoletti, E., Sicard, P., Sitch, S., Vitale, M., 2016. Comparing concentration-based (AOT40) and stomatal uptake (POD_Y) metrics for ozone risk assessment to European forests. Glob. Chang. Biol. 22 (4), 1608–1627. https://doi.org/10.1111/gcb.13138.

Anav, A., Proietti, C., Menut, L., Carnicelli, S., Marco, A.D., Paoletti, E., 2018. Sensitivity of stomatal conductance to soil moisture: implications for tropospheric ozone. Atmos. Chem. Phys. 18 (8), 5747–5763. https://doi.org/10.5194/acp–18–5747–2018.

Anav, A., De Marco, A., Savi, F., Sicard, P., Sitch, S., Vitale, M., Paoletti, E., 2019. Growing season extension affects ozone uptake by forests in Europe. Sci. Total Environ. 669, 1043–1052.

Araminiene, V., Sicard, P., Anav, A., Agathokleous, E., Stakenas, V., De Marco, A., Varnagirytė–Kabašinskienė, I., Paoletti, E., Girgždienė, R., 2019. Trends and inter–relationships of ground–level ozone metrics and forest health in Lithuania. Sci. Total Environ. 658, 1265–1277. https://doi.org/10.1016/j.scitotenv.2018.12.092.

Augustaitis, A., Bytnerowicz, A., 2008. Contribution of ambient ozone to Scots pine defoliation and reduced growth in the Central European forests: a Lithuanian case study. Environ. Pollut. 155 (3), 436–445. https://doi.org/10.1016/j.envpol.2008.01.042.

Augustaitis, A., Sopauskiene, D., Bauziene, I., 2010. Direct and indirect effects of regional air pollution on tree crown defoliation. Balt. For. 16 (1), 23–34.

Badea, O., 2008. Manual on Methodology for Long–Term Monitoring of Forest Ecosystems Status under Air Pollution and Climate Change Influence. Editura Silvică, Bucharest.

Badea, O., Tanase, M., Georgeta, J., Anisoara, L., Peiov, A., Uhlirova, H., Pajtikc, J., Wawrzoniakd, J., Shparyk, Y., 2004. Forest health status in the Carpathian Mountains over the period 1997–2001. Environ. Pollut. 130 (1), 93–98. https://doi.org/10.1016/j.envpol.2003.10.024.

Balducci, L., Cuny, H.E., Rathgeber, C.B.K., Deslauriers, A., Giovannelli, A., Rossi, S., 2016. Compensatory mechanisms mitigate the effect of warming and drought on wood formation. Plant Cell Environ. 39, 1338–1352. https://doi.org/10.1111/pce.12689.

Bertini, G., Amoriello, T., Fabbio, G., Piovosi, M., 2011. Forest growth and climate change: evidences from the ICP Forest intensive monitoring in Italy. iForest 4, 262.267. https://doi.org/10.3832/ifor0596–004.

Bertini, G., Amoriello, T., Piovosi, M., Fabbio, G., 2013. Alcune evidenze dal monitoraggio intensivo delle foreste italiane. L'accrescimento radiale degli alberi come indice di risposta ai disturbi e le sue relazioni con la struttura del soprassuolo. Forest@ 10, 68–78. https://doi.org/10.3832/efor1010–010.

Beuker, E., Raspe, S., Bastrup-Birk, A., Preuhsler, T., Fleck, S., 2016. Part VI: phenological observations., In: UNECE ICP Forests Programme Co-ordinating Centre (Ed.): Manual on Methods and Criteria for Harmonized Sampling, Assessment, Monitoring and Analysis of the Effects of Air Pollution on Forests. Thünen Institute of Forest Ecosystems, Eberswalde, Germany, 18 pp.. [http://www.icpforests.org/Manual.htm]. ISBN: 978–3–86576–162–0.

Braun, S., Achermann, B., De Marco, A., Pleijel, H., Karlsson, P.E., Rihm, B., Schindler, C., Paoletti, E., 2017. Epidemiological analysis of ozone and nitrogen impacts on vegetation–critical evaluation and recommendations. Sci. Total Environ. 603, 785–792. https://doi.org/10.1016/j.scitotenv.2017.02.225.

Büker, P., Feng, Z., Uddling, J., Briolat, A., Alonso, R., Braun, S., Elvira, S., Gerosa, G., Karlsson, P.E., Le Thiech, D., Marzuoli, R., Mills, G., Oksanen, E., Wieser, G., Wilkinson, M., Emberson, L.D., 2015. New flux based dose–response relationships for ozone for European forest tree species. Environ. Pollut. 206, 163–174. https://doi.org/10.1016/j.envpol.2015.06.033.

Caldwell, M.M., Dawson, T.E., Richards, J.H., 1998. Hydraulic lift: consequences of water efflux from the roots of plants. Oecologia 1132, 151–161. https://doi.org/10.1007/s004420050363.

CLRTAP, 2017. Mapping critical levels for vegetation, chapter III of manual on methodologies and criteria for modelling and mapping critical loads and levels and air pollution effects, risks and trends. UNECE Convention on Long–Range Transboundary Air Pollution http://icpmapping.org/Publications_CLRTAP, Accessed date: 16 July 2018.

Cocozza, C., Palombo, C., Tognetti, R., La Porta, N., Anichini, M., Giovannelli, A., Emiliani, G., 2016. Monitoring intra–annual dynamics of wood formation with microcores and dendrometers in *Picea abies* at two different altitudes. Tree Physiol. 36, 832–846. https://doi.org/10.1093/treephys/tpw009.

Cooper, O.R., Parrish, D.D., Ziemke, J., Cupeiro, M., Galbally, I.E., Gilge, Horowitz, S.L., Jensen, N.R., Lamarque, J.-F., Naik, V., Oltmans, S.J., Schwab, J., Shindell, D.T., Thompson, A.M., Thouret, V., Wang, Y., Zbinden, R.M., 2014. Global distribution and trends of tropospheric ozone: an observation–based review. Elem. Sci. Anth. 2, 29. https://doi.org/10.12952/journal.elementa.000029.

De Marco, A., Sicard, P., Vitale, M., Carriero, G., Renou, C., Paoletti, E., 2015. Metrics of ozone risk assessment for Southern European forests: canopy moisture content as a potential plant response indicator. Atmos. Environ. 120, 182–190. https://doi.org/10.1016/j.atmosenv.2015.08.071.

De Marco, A., Sicard, P., Fares, S., Tuovinen, J.P., Anav, A., Paoletti, E., 2016. Assessing the role of soil water limitation in determining the Phytotoxic Ozone Dose (POD_Y) thresholds. Atmos. Environ. 147, 88–97. https://doi.org/10.1016/j.atmosenv.2016.09.066.

De Marco, A., Vitale, M., Popa, I., Anav, A., Badea, O., Silaghi, D., Leca, S., Screpanti, A., Paoletti, E., 2017. Ozone exposure affects tree defoliation in a continental climate. Sci. Total Environ. 596, 396–404. https://doi.org/10.1016/j.scitotenv.2017.03.135.

De Marco, A., Proietti, C., Anav, A., Ciancarella, L., D'Elia, I., Fares, S., Fornasier, M–.F., Fusaro, L., Gualtieri, M., Manes, F., Marchetto, A., Mircea, M., Paoletti, E., Piersanti, A., Rogora, M., Salvati, L., Salvatori, E., Screpanti, A., Vialetto, G., Vitale, M., Leonardi, C., 2019. Impacts of air pollution on human and ecosystem health, and implications for the National Emission Ceilings Directive: insights from Italy. Environ. Int. 125, 320–333.

Deslauriers, A., Morin, H., Bégin, Y., 2003. Cellular phenology of annual ring formation of *Abies balsamea* in the Québec boreal forest (Canada). Can. J. For. Res. 33, 190–200. https://doi.org/10.1139/x02–178.

Díaz-de-Quijano, M., Penuelas, J., Ribas, A., 2009. Increasing interannual and altitudinal ozone mixing ratios in the Catalan Pyrenees. Atmos. Environ. 43 (38), 6049–6057. https://doi.org/10.1016/j.atmosenv.2009.08.035.

Dobbertin, M., Rigling, A., 2006. Pine mistletoe (Viscum album ssp. austriacum) contributes to Scots pine (Pinus sylvestris) mortality in the Rhone valley of Switzerland. For. Pathol. 36, 309–322.

Eichhorn, J., Roskams, P., Pototic, N., Timmerman, V., Ferretti, M., Mues, V., Szepesi, A., Durrant, D., Seletcovic, I., Schöck, H.W., Nevalainen, S., Bussotti, F., Garcia, P., Wulff, S., 2016. Part IV: visual assessment of crown condition and damaging agents. In: UNECE ICP Forests Programme Coordinating Centre (Ed.): Manual on Methods and Criteria for Harmonized Sampling, Assessment, Monitoring and Analysis of the Effects of Air Pollution on Forests. Thünen Institute of Forest Ecosystems, Eberswalde, Germany, 54 pp.. [http://www.icp-forests.org/Manual.htm].

Emberson, L.D., Ashmore, M.R., Cambridge, H.M., Simpson, D., Tuovinen, J.P., 2000. Modelling stomatal ozone flux across Europe. Environ. Pollut. 109 (3), 403–413. https://doi.org/10.1016/S0269-7491(00)00043-9.

Fabbio, G., Bertini, G., Calderisi, M., Ferretti, M., 2008. Status and trend of tree growth and mortality rate at the Conecofor plots, 1997–2004. Annali CRA–Centro di ricerca per la selvicoltura, Arezzo, Spec. Issue. vol. 34, pp. 11–20.

Fan, J., McConkey, B., Wang, H., Janzen, H., 2016. Root distribution by depth for temperate agricultural crops. Field Crop Res. 189, 68–74. https://doi.org/10.1016/j.fcr.2016.02.013.

FAO, 1998. World Reference Base for Soil Resources. vol. 3. Food & Agriculture Organization of the United Nations, Rome ISSN 0532–0488.

Ferretti M, Fischer R, Mues V, Granke O, Lorenz M, Seidling W, 2017: Part II: basic design principles for the ICP forests monitoring networks. In: UNECE ICP Forests Programme Co-ordinating Centre (Ed.): Manual on Methods and Criteria for Harmonized Sampling, Assessment, Monitoring and Analysis of the Effects of Air Pollution on Forests. Thünen Institute of Forest Ecosystems, Eberswalde, Germany, 21 p + Annex. [http://www.icp-forests.net/page/icp-forests-manual].

Finér, L., Ohashi, M., Noguchi, K., Hirano, T., 2011. Fine root production and turnover in forest ecosystems in relation to stand and environmental characteristics. For. Ecol. Manag. 262, 2008–2023. https://doi.org/10.1016/j.foreco.2011.08.042.

Gaines, K.P., Stanley, J.W., Meinzer, F.C., McCulloh, K.A., Woodruff, D.R., Chen, W., Adams, T.S., Lin, H., Eissenstat, D.M., 2015. Reliance on shallow soil water in a mixed–hardwood forest in central Pennsylvania. Tree Physiol. 36, 444–458. https://doi.org/10.1093/treephys/tpv113.

Giovannelli, A., Deslauriers, A., Fragnelli, G., Scaletti, L., Castro, G., Rossi, S., Crivellaro, A., 2007. Evaluation of drought response of two poplar clones (*Populus*×*canadensis* Mönch 'I–214'and *P. deltoides* Marsh.'Dvina') through high resolution analysis of stem growth. J. Exp. Bot. 58 (10), 2673–2683. https://doi.org/10.1093/jxb/erm117.

Girgždienė, R., Serafinavičiūtė, B., Stakėnas, V., Byčenkienė, S., 2009. Ambient ozone concentration and its impact on forest vegetation in Lithuania. AMBIO J. Hum. Environ. 38 (8), 432–436. https://doi.org/10.1579/0044–7447–38.8.432.

Granier, A., Reichstein, M., Bréda, N., Janssens, I.A., Falge, E., Ciais, P., Gru¨nwald, T., Aubinet, M., Berbigier, P., Bernhofer, C., Buchmann, N., Facini, O., Grassi, G., Heinesch, B., Ilvesniemi, H., Keronen, P., Knohl, A., Ko¨stne, B., Lagergren, F., Lindroth, A., Longdoz, B., Loustau, D., Mateus, J., Montagnani, L., Nyst, C., Moors, E., Papale, D., Peiffer, M., Pilegaard, K., Pita, G., Pumpanen, J., Rambal, S., Rebmann, C., Rodrigues, A., Seufert, G., Tenhunen, J., Vesala, T., Wang, Q., 2007. Evidence for soil water control on carbon and water dynamics in European forests during the extremely dry year: 2003. Agric. For. Meteorol. 143 (1–2), 123–145. https://doi.org/10.1016/j.agrformet.2006.12.004.

Günthardt-Goerg, M.S., Vollenweider, P., 2007. Linking stress with macroscopic and microscopic leaf response in trees: new diagnostic perspectives. Environ. Pollut. 147 (3), 467–488. https://doi.org/10.1016/j.envpol.2006.08.033.

Hoshika, Y., Paoletti, E., Omasa, K., 2012a. Parameterization of *Zelkova serrata* stomatal conductance model to estimate stomatal ozone uptake in Japan. Atmos. Environ. 55, 271–278. https://doi.org/10.1016/j.atmosenv.2012.02.083.

Hoshika, Y., Watanabe, M., Inada, N., Koike, T., 2012b. Modeling of stomatal ozone conductance for estimating ozone uptake of *Fagus crenata* under experimentally enhanced free–air ozone exposure. Water Air Soil Pollut. 223, 3893–3901. https://doi.org/10.1007/s11270–012–1158–9.

Hoshika, Y., Watanabe, M., Inada, N., Mao, Q., Koike, T., 2013. Photosynthetic response of early and late leaves of white birch (*Betula platyphylla* var. *japonica*) grown under free–air ozone exposure. Environ. Pollut. 182, 242–247. https://doi.org/10.1016/j.envpol.2013.07.033.

Hoshika, Y., Moura, B., Paoletti, E., 2018a. Ozone risk assessment in three oak species as affected by soil water availability. Environ. Sci. Pollut. Res. 25, 8125–8136. https://doi.org/10.1007/s11356–017–9786–7.

Hoshika, Y., Carrari, E., Zhang, L., Carriero, G., Pignatelli, S., Fasano, G., Materassi, A., Paoletti, E., 2018b. Testing a ratio of photosynthesis to O_3 uptake as an index for assessing O_3–induced foliar visible injury in poplar trees. Environ. Sci. Pollut. Res. 25, 8113–8124. https://doi.org/10.1007/s11356–017–9475–6.

Jackson, R.B., Canadell, J., Ehleringer, J.R., Mooney, H.A., Sala, O.E., Schulze, E.D., 1996. A global analysis of root distributions for terrestrial biomes. Oecologia 108, 389–411. https://doi.org/10.1007/BF00333714.

Krupa, S., McGrath, M.T., Andersen, C.P., Booker, F.L., Burkey, K.O., Chappelka, A.H., Chevone, B.I., Pell, E.J., Zilinskas, B.A., 2001. Ambient ozone and plant health. Plant Dis. 85 (1), 4–12. https://doi.org/10.1094/PDIS.2001.85.1.4.

Langner, J., Engardt, M., Baklanov, A., Christensen, J.H., Gauss, M., Geels, C., Hedegaard, G.B., Nuterman, R., Simpson, D., Soares, J., Sofiev, M., Wind, P., Zakey, A., 2012. A multi–model study of impacts of climate change on surface ozone in Europe. Atmos. Chem. Phys. 1221, 10423–10440. https://doi.org/10.5194/acp–12–10423–2012.

Lefohn, A.S., Shadwick, D., Oltmans, S.J., 2010. Characterizing changes in surface ozone levels in metropolitan and rural areas in the United States for 1980–2008 and 1994–2008. Atmos. Environ. 44 (39), 5199–5210. https://doi.org/10.1016/j.atmosenv.2010.08.049.

Lefohn, A.S., Malley, C.S., Smith, L., Wells, B., Hazucha, M., Simon, H., Naik, V., Mills, G., Schultz, M.G., Paoletti, E., De Marco, A., Xu, X., Zhang, L., Wang, T., Neufeld, H.S., Musselman, R.C., Tarasick, D., Feng, Z., Tang, H., Kobayashi, K., Sicard, P., Solberg, S., Gerosa, G., 2018. Tropospheric ozone assessment report: global ozone metrics for climate change, human health, and crop/ecosystem research. Elem. Sci. Anth. 1, 6–28 http://hdl.handle.net/11250/2496199.

Li, P., De Marco, A., Feng, Z., Anav, A., Zhou, D., Paoletti, E., 2018. Nationwide ground–level ozone measurements in China suggest serious risks to forests. Environ. Pollut. 237, 803–813. https://doi.org/10.1016/j.envpol.2017.11.002.

Matyssek, R., Wieser, G., Ceulemans, R., Rennenberg, H., Pretzsch, K., Häberle, K.H., Löw, M., Nunn, A.J., Werner, H., Wipfler, P., Oßwald, W., Nikolova, P., Hanke, D.E., Kraigher, H., Tausz, M., Bahnweg, G., Kitao, M., Dieler, J., Sandermann, H., Herbinger, K., Grebenc, T., Blumenröther, M., Deckmyn, G., Grams, T.E.E., Heerdt, C., Leuchner, M., Fabian, P., Häberle, K.H., 2010. Enhanced ozone strongly reduces carbon sink strength of adult beech (*Fagus sylvatica*) a resume from the free–air fumigation study at Kranzberg forest. Environ. Pollut. 158 (8), 2527–2532. https://doi.org/10.1016/j.envpol.2010.05.009.

McLaughlin, S.B., Downing, D.J., 1996. Interactive effects of ambient ozone and climate measured on growth of mature loblolly pine trees. Can. J. For. Res. 26 (4), 670–681. https://doi.org/10.1139/x26–077.

McLaughlin, S.B., Nosal, M., Wullschleger, S.D., Sun, G., 2007. Interactive effects of ozone and climate on tree growth and water use in a southern Appalachian forest in the USA. New Phytol. 174 (1), 109–124. https://doi.org/10.1111/j.1469–8137.2007.02018.x.

Mills, G., Pleijel, H., Braun, S., Büker, P., Bermejo, V., Calvo, E., Danielsson, H., Emberson, L., Fern andez, I.G., Grünhage, L., Harmens, H., Hayes, F., Karlsson, P.–.E., Simpson, D., 2011. New stomatal flux–based critical levels for ozone effects on vegetation. Atmos. Environ. 45, 5064e5068. https://doi.org/10.1016/j.atmosenv.2011.06.009.

Mills, G., Pleijel, H., Malley, C.S., Sinha, B., Cooper, O.R., Schultz, M.G., Neufeld, H.S., Simpson, D., Sharps, S., Feng, Z., Gerosa, G., Harmens, H., Kobayashi, K., Saxena, P., Paoletti, E., Sinha, V., Xu, X., 2018. Tropospheric Ozone Assessment Report: present–day tropospheric ozone distribution and trends relevant to vegetation. Elem. Sci. Anth. 6. https://doi.org/10.1525/elementa.302.

Nunn, A.J., Kozovits, A.R., Reiter, I.M., Heerdt, C., Leuchner, M., Lutz, C., Liu, X., Low, M., Winkler, J.B., 2005. Comparison of ozone uptake and sensitivity between a phytotron study with young beech and a field experiment with adult beech (Fagus sylvatica). Environ. Pollut. 137, 494–506.

Oberhuber, W., Gruber, A., Kofler, W., Swidrak, I., 2014. Radial stem growth in response to microclimate and soil moisture in a drought–prone mixed coniferous forest at an inner Alpine site. Eur. J. For. Res. 133, 467–479. https://doi.org/10.1007/s10342–013–0777–z.

Paoletti, E., 2006. Impact of ozone on Mediterranean forests: a review. Environ. Pollut. 1442, 463–474. https://doi.org/10.1016/j.envpol.2005.12.051.

Paoletti, E., Manning, W.J., 2007. Toward a biologically significant and usable standard for ozone that will also protect plants. Environ. Pollut. 150, 85–95. https://doi.org/10.1016/j.envpol.2007.06.037.

Paoletti, E., Bytnerowicz, A., Schaub, M., 2007. Key studies on air pollution and climate change impacts on forests: an introduction. Environ. Monit. Assess. 128, 1–3. https://doi.org/10.1007/s10661–006–9408–1.

Paoletti, E., Ferrara, A.M., Calatayud, V., Cerveró, J., Giannetti, F., Sanz, M.J., Manning, W.J., 2009. Deciduous shrubs for ozone bioindication: *Hibiscus syriacus* as an example. Environ. Pollut. 157 (3), 865–870. https://doi.org/10.1016/j.envpol.2008.11.009.

Paoletti, E., De Marco, A., Beddows, D.C., Harrison, R.M., Manning, W.J., 2014. Ozone levels in European and USA cities are increasing more than at rural sites, while peak values are decreasing. Environ. Pollut. 192, 295–299. https://doi.org/10.1016/j.envpol.2014.04.040.

Paoletti, E., Materassi, A., Fasano, G., Hoshika, Y., Carriero, G., Silaghi, D., Badea, O., 2017. A new–generation 3D ozone FACE (Free Air Controlled Exposure). Sci. Total Environ. 575, 1407–1414. https://doi.org/10.1016/j.scitotenv.2016.09.217.

Paoletti, E., De Marco, A., Anav, A., Gasparini, P., Pompei, E., 2018. Five-year volume growth of European beech does not respond to ozone pollution in Italy. Environ. Sci. Pollut. Res. 25, 8233–8239. https://doi.org/10.1007/s11356-017-9264-2.

Proietti, C., Anav, A., De Marco, A., Sicard, P., Vitale, M., 2016. A multi–sites analysis on the ozone effects on Gross Primary Production of European forests. Sci. Total Environ. 556, 1–11. https://doi.org/10.1016/j.scitotenv.2016.02.187.

Rytter, R.M., Hansson, A.C., 1996. Seasonal amount, growth and depth distribution of fine roots in an irrigated and fertilized *Salix viminalis* L. plantation. Biomass Bioenergy 112–3, 129–137. https://doi.org/10.1016/0961–9534(96)00023–2.

Sanz, M.J., Calatayud, V., 2018. Ozone injury in European forest species. http://www.ozoneinjury.org, Accessed date: 1 December 2018.

Schaub, M., Calatayud, V., Ferretti, M., Brunialti, G., Lövblad, G., Krause, G., Sanz, M.J., 2010. Monitoring of ozone injury. Manual part X. 22 pp. Manual on Methods and Criteria for Harmonized Sampling, Assessment, Monitoring and Analysis of the Effects of Air Pollution on Forests. UNECE ICP Forests Programme, Hamburg ISBN: 978–3–926301–03–1.

Schaub, M., Calatayud, V., Ferretti, M., Brunialti, G., Lövblad, G., Krause, G., Sanz, M.J., 2016. Part VIII: monitoring of ozone injury. In: UNECE ICP Forests Programme Co-ordinating Centre (Ed.), Manual on Methods and Criteria for Harmonized Sampling, Assessment, Monitoring and Analysis of the Effects of Air Pollution on Forests. Thünen Institute of Forest Ecosystems, Eberswalde, Germany, 14 p. + Annex [http://www.icp-forests.org/manual.htm].

Schenk, H.J., Jackson, R.B., 2002. The global biogeography of roots. Ecol. Monogr. 72, 311–328. https://doi.org/10.1890/0012–96152002)072[0311:TGBOR]2.0.CO;2.

Sicard, P., Dalstein–Richier, L., 2015. Health and vitality assessment of two common pine species in the context of climate change in southern Europe. Environ. Res. 137, 235–245. https://doi.org/10.1016/j.envres.2014.12.025.

Sicard, P., De Marco, A., Troussier, F., Renou, C., Vas, N., Paoletti, E., 2013. Decrease in surface ozone concentrations at Mediterranean remote sites and increase in the cities. Atmos. Environ. 79, 705–715. https://doi.org/10.1016/j.atmosenv.2013.07.042.

Sicard, P., De Marco, A., Dalstein–Richier, L., Tagliaferro, F., Renou, C., Paoletti, E., 2016a. An epidemiological assessment of stomatal ozone flux–based critical levels for visible ozone injury in Southern European forests. Sci. Total Environ. 541, 729–741. https://doi.org/10.1016/j.scitotenv.2015.09.113.

Sicard, P., Serra, R., Rossello, P., 2016b. Spatiotemporal trends in ground–level ozone concentrations and metrics in France over the time period 1999–2012. Environ. Res. 149, 122–144.

Simpson, D., Ashmore, M.R., Emberson, L., Tuovinen, J.P., 2007. A comparison of two different approaches for mapping potential ozone damage to vegetation. A model study. Environ. Pollut. 146, 715–725.

Tagliaferro, F., Ferrara, A.M., Spaziani, F., Viotto, E., 2005. Sintomi fogliari di tipo ozone like su vegetazione spontanea e ornamentale in Piemonte. Linea Ecol. 27, 47–53.

Traversari, S., Francini, A., Traversi, M.L., Emiliani, G., Sorce, C., Sebastiani, L., Giovannelli, A., 2018. Can sugar metabolism in the cambial region explain the water deficit tolerance in poplar? J. Exp. Bot. 69, 4083–4097.

Tutin, T.G., Heywood, V.H., Burges, N.A., Moore, D.M., Valentine, D.H., Walters, S.M., Webb, D.A., 1993. Flora Europaea. 2nd edn. University Press, Cambridge, UK.

UN/ECE – ICP Forests, 2010. Manual on Methods and Criteria for Harmonized Sampling, Assessment, Monitoring and Analysis of the Effects of Air Pollution on Forests Part II Visual Assessment of Crown Condition. Hamburg. http://icp-forests.net/page/icp-forests-manual.

Yuan, X., Calatayud, V., Gao, F., Fares, S., Paoletti, E., Tian, Y., 2016. Interaction of drought and ozone exposure on isoprene emission from extensively cultivated poplar. Plant cell Environ. 39, 2276–2287.

Zhang, L., Hoshika, Y., Carrari, E., Badea, O., Paoletti, E., 2018. Ozone risk assessment is affected by nutrient availability: evidence from a simulation experiment under free air controlled exposure (FACE). Environ. Pollut. 238, 812–822. https://doi.org/10.1016/j.envpol.2018.03.102.

Zweifel, R., Haeni, M., Buchmann, N., Eugster, W., 2016. Are trees able to grow in periods of stem shrinkage? New Phytol. 211, 839–849. https://doi.org/10.1111/nph.13995.